

Basic relations between physical parameters of Wolf–Rayet stars

D. Schaerer and A. Maeder

Geneva Observatory, CH-1290 Sauverny, Switzerland

Received May 15, accepted June 1, 1992

Abstract. Based on new grids of stellar models by Schaller et al. (1992) we study the physical parameters of Wolf-Rayet stars, which can be expressed as a function of one main parameter, the mass of the bare stellar core, and the chemical composition to a smaller extent. We show the existence of simple relations between mass, luminosity, radius and effective temperature determined at optical depth $\tau = 2/3$ in the wind. Analytical expressions and graphical representations of these relations are given. In addition our evolutionary models predict a relation between the initial ZAMS mass and the luminosity of the WNL and WNE stars. New indication for mass-dependent mass loss rates as found by Langer (1989b) is also obtained from the correlation of surface mass flux and temperature given by Howarth & Schmutz (1992) and the relations obtained in this work.

WC and WO stars offer the unique opportunity to study the abundance of the products of partial He-burning, carbon and oxygen. Thus they provide us with valuable information about massive star evolution and the underlying physics, especially mass loss in post MS phases and the efficiency of convection. In this work C and O surface abundances predicted by evolutionary models using commonly adopted mass loss rates and enhanced post MS mass loss rates are compared to observations. The influence of overshooting and adopted nuclear reaction rates is discussed. All observations of surface abundances and the observed number ratios of different WR stars lead us to suggest that massive stars have larger post main-sequence mass loss rates than commonly adopted.

Key words: stars: evolution – stars: Wolf-Rayet – stars: abundances – stars: mass loss

1. Introduction

The identification of Wolf-Rayet (WR) stars as objects in late evolutionary stages of massive stars, which have lost most of their H-rich outer layers in previous phases is quite generally accepted (cf. Lamers et al. 1991). Independently of their previous evolution, stars in the WR phase possess the following basic structure: WR stars are bare, chemically quasi-homogeneous stellar cores with central He-burning (cf. Maeder 1983). The so called late WN stars (WNL) are an exception: the majority of them still contain a certain amount of hydrogen in their envelope and are likely to possess a hydrogen burning shell. Thus WNL stars behave somehow differently than the other WR stars. In early WN stars

(WNE), WC and WO stars, however, hydrogen is nearly or completely absent (cf. Hamann et al. 1991; Nugis 1991), the star is composed of a quasi-homogeneous He–C–O mixture and its nuclear energy source is core helium burning.

The relatively simple inner structure of WR stars with a large convective core, a small radiative envelope and chemical quasi-homogeneity gives raise to a number of relations for the different stellar parameters, as the mass, luminosity, radius (cf. Maeder 1983; Langer 1989a) and surface temperature. Hence these relations are independent of the rather uncertain mass loss rates and the precise history of the stars.

On the other hand, the effective temperature of WR stars is largely influenced by the effects of the stellar winds, i. e. by their mass loss. The same holds for the surface abundances of products of the CNO cycles and He-burning reactions, since these abundances are mainly determined by the time at which the stellar envelope will be peeled off to exhibit the bare core. Although the huge mass loss rate \dot{M} of WR stars does not seem to be driven by radiation pressure alone (cf. Schmutz & Schaerer 1992) a dependence of \dot{M} on the luminosity or equivalently on the mass (due to the existence of a simple mass–luminosity relation) has been suggested on both theoretical and observational grounds by Maeder (1985) and Langer (1989b), and is supported by evolutionary models of Maeder (1991), which show remarkable agreement for the relative numbers of WR stars over various metallicities if mass-dependent mass loss rates are applied. To a smaller extent \dot{M} may also depend on the chemical composition. Thus all properties of WR stars, including the effective temperature determined at a certain optical depth in the wind, can be expressed as a function of one main parameter, the mass of the bare core.

In this paper we derive several relations for WR stars between mass, luminosity, radius, surface temperature and effective temperature obtained from new grids of stellar models by Schaller et al. (1992). These are given in Section 2. Surface abundances of He, C and O of WC/WO stars, their dependence on mass loss and comparisons to observations is the object of Sect. 3. The conclusions are drawn in Sect. 4.

2. Relations between fundamental parameters of WR stars

2.1. Input physics of WR models

The WR models used in this work are taken from the results by Schaller et al. (1992) at solar metallicity. We refer to them for a detailed description of the input physics. We only list some of their improvements which are of importance to this work are:

– New OPAL radiative opacities.

Send offprint requests to: D. Schaerer

- Update of nuclear cross-sections.
- Detailed treatment of partial ionisation for the main heavy elements.
- Determination of T_{eff} in the optically thick stellar wind in the framework of the radiation-driven wind theory.
- Changes in the algorithms to compute the chemical changes in convective cores with greater accuracy.
- New calibration of convective overshooting parameter.

The changes brought about by these improvements will be commented if necessary.

2.2. Grid of WR models used, mass loss rates

In the models by Schaller et al. the formation of WR stars occurs for the models with initial $M \geq 40 M_{\odot}$. Hence our study is based on their models with initial masses of 40, 60, 85 and $120 M_{\odot}$. The mass loss rates (called “standard” mass loss henceforth) used in these models are given in their paper. The mass loss rate applied during the He-burning phase, especially during the WR phases is of special interest for this work. For the WNL phase, an average mass loss of $4 \cdot 10^{-5} M_{\odot} \text{yr}^{-1}$ is adopted. The mass-dependent mass loss rates found by Langer (1989b) are adopted in the WNE and WC/WO stages. New indications for this type of dependence will be discussed below. The models by Schaller et al. have also been computed with twice the standard mass loss in all post main-sequence (post MS) stages. These will henceforth be referenced by “high” mass loss.

2.3. Definitions

The WNL, WNE, WC and WO stars are defined by spectroscopic properties. The correspondence to precise evolutionary stages in theoretical models, although relatively clear in general, is nevertheless subject to some uncertainties and exceptions. Here, for purpose of clarity, we adopt the general scheme which results from abundance determinations and their comparison to theoretical values (cf. Willis 1991). As mentioned above, WNL stars generally have some hydrogen present, and will be considered as such in the models. In WNE stars hydrogen is generally absent and they do not yet show the products of He-burning. Thus the correspondence with models is relatively unambiguous. The passage from the WNE to the WC phase is marked by an relatively abrupt change of the surface abundances with the appearance of 3α -products. The physical reasons for the separation of these phases was given by Maeder (1983). Since the transition to the WO phase is not accompanied by such a structural change, but can be determined by the surface O/C ratio (cf. Smith & Maeder 1991), the separation between WC and WO stars in evolutionary models is smooth. Therefore these phases will be referenced by WC/WO. The relations derived below apply to both the WNE and WC/WO phase and until the end of He-burning unless stated differently.

In order to avoid any confusion we recall several expressions (cf. Schaller et al. 1992). The stellar radius or core radius R_{\star} is the radius of the hydrostatic stellar model without taking the wind into account. The temperature at this point is called the (core) surface temperature T_{\star} of the star. The effective temperature T_{eff} is defined at the optical-depth radius where the flux weighted mean opacity reaches $\tau(r) = 2/3$.

2.4. Mass – luminosity relation

As already noted by several authors (Maeder 1983; Maeder & Meynet 1987; Langer 1989a) WNE and WC/WO stars obey a simple mass-luminosity relation. This is explained by the simple structure of these stars and is essentially described by

$$L = \frac{4\pi G c}{\kappa} (1 - \beta) M \quad (1)$$

(Chandrasekhar 1939). Since the opacity is almost pure electron scattering and radiation pressure dominates in such massive stars, L is rather insensitive to changes of the chemical composition. As already stated by Langer (1989a) this explains the well defined mass-luminosity relation.

Figure 1 shows this relation obtained from our WR models. The models with higher mass loss rates (twice the “standard” value) reach lower masses at the end of He-burning. The scatter among the models is due to differences in the evolutionary stages at the same actual WR mass. Different evolutionary stages have distinct central helium contents, i. e. different mean molecular weights μ_c at the stellar centre. The higher μ_c , the larger is the luminosity of the corresponding model. This is explained as follows: If radiation pressure dominates $\beta \sim 1/\mu$, hence L rises with μ_c .

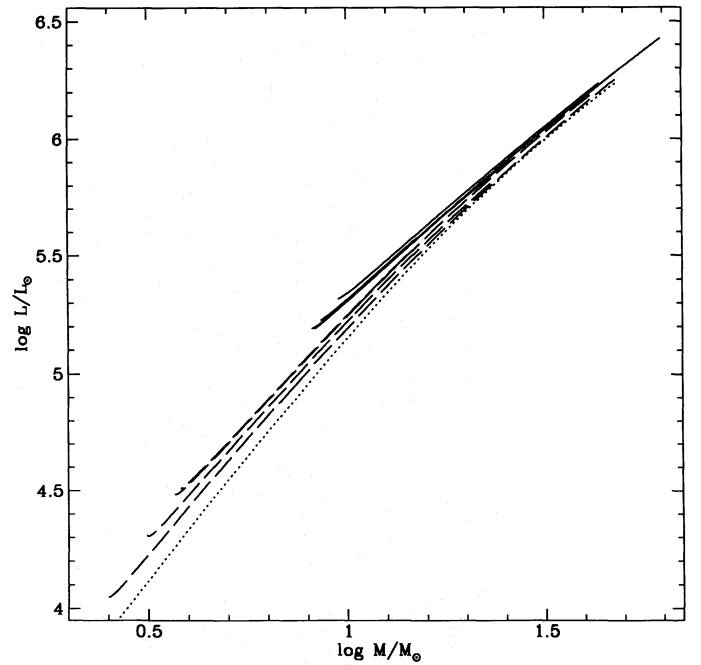


Fig. 1. Mass–luminosity relation for WNE and WC/WO stars. Models with “standard” mass loss (solid lines) and high \dot{M} (long dashed lines). The relation obtained by Langer (1989a) for homogeneous models taking surface abundances of our $120 M_{\odot}$ model (dotted line) is shown as a comparison

A linear fit to the data shown in Fig. 1 gives:

$$\log \frac{L}{L_{\odot}} = 3.4949 + 1.7267 \log \frac{M}{M_{\odot}} \quad (2)$$

A better fit is obtained with an accuracy of ± 0.1 dex by:

$$\log \frac{L}{L_{\odot}} = 3.0321 + 2.6950 \log \frac{M}{M_{\odot}} - 0.4610 \left(\log \frac{M}{M_{\odot}} \right)^2 \quad (3)$$

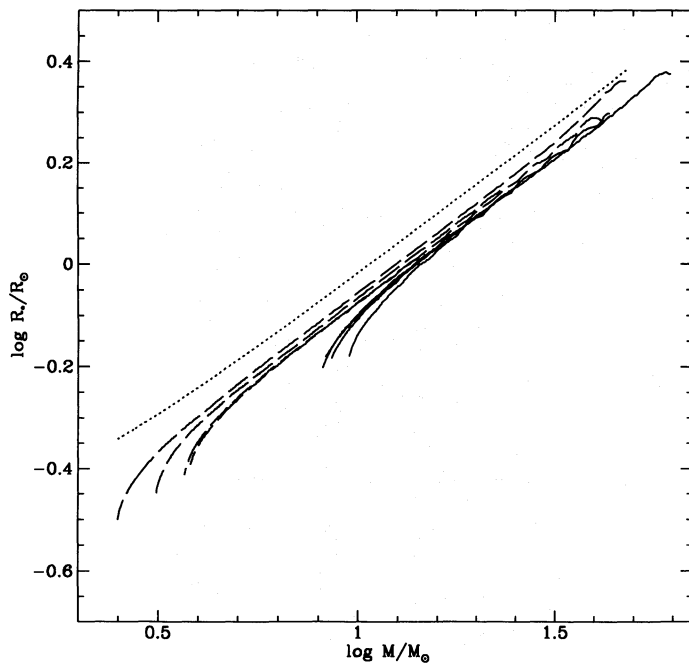


Fig. 2. Mass – core radius relation for WC/WO stars. Models with “standard” mass loss (solid lines) and high \dot{M} (long dashed lines). The dotted line gives the relation obtained by Langer (1989a)

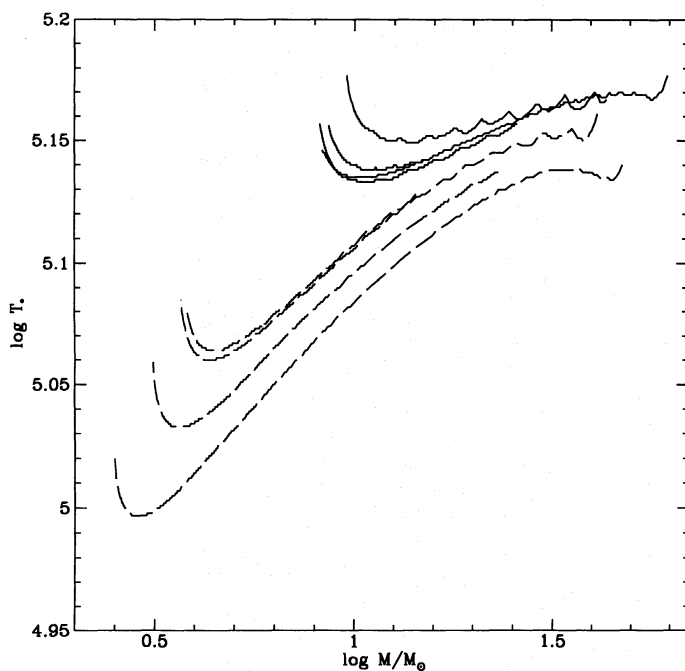


Fig. 3. Surface temperature of WC/WO stars. Models with “standard” mass loss (solid lines) and high \dot{M} (long dashed lines)

The relation derived by Maeder & Meynet (1987) from WR stars in the mass range $10M_{\odot} \lesssim M_{\text{WR}} \lesssim 70M_{\odot}$ agrees well with our relation in this mass range. The mass luminosity relation for WC stars given by Langer (1989a) is also given in Fig. 1 for the $120M_{\odot}$ model with high mass loss. As Langer showed, the properties of *homogeneous* WR stars are determined by their mass and surface chemical composition. The comparison with our relation shows the differences obtained between homogeneous models and evolutionary models. In this precise case, our $120M_{\odot}$ model is homogeneous at the beginning of the WC stage but reaches the end of He-burning with a surface helium abundance $Y_s = 0.3$. Thus the relations obtained from entirely homogeneous models give a lower limit to the luminosity of evolutionary models. This is consistent with the fact that L rises with μ_c .

Langer (1989a) obtained relations that differ between WNE and WC/WO stars. This is due to his definition of WNE stars as pure (homogeneous) helium stars while our models show a continuity in the course of He-processing.

The tracks with higher \dot{M} reach down to smaller mass i. e. lower luminosities at the end of He-burning for WC stars, while the luminosity in the WNL and WNE phase is hardly affected by uncertain mass loss rates (cf. Section 2.11).

2.5. Mass – radius relation

Figure 2 shows the mass-radius relation for WC/WO stars. During He-burning the radii of WR stars decrease while the masses are declining. At a given WR mass the star with a higher molecular weight has a smaller radius. Towards the end of He-burning a more rapid core contraction occurs in order to maintain the luminosity. The decrease of the nuclear energy production from the 3α -process, which is proportional to Y^3 , requires this contraction to enable $^{12}\text{C}(\alpha, \gamma)^{16}\text{O}$ to produce the emergent luminosity. This was already found in Langer’s (1989a) models.

The radii of our WNE models are slightly smaller than the ones for the WC/WO stars but are within the spread shown in Fig. 2.

If we exclude the part where the more rapid contraction occurs, we obtain the following linear fit for the WNE, WC and WO stars, with an accuracy of ± 0.05 dex:

$$\log \frac{R_{\star}}{R_{\odot}} = -0.6629 + 0.5840 \log \frac{M}{M_{\odot}}. \quad (4)$$

The radii we obtain are $\approx 0.05 - 0.1$ dex smaller than the ones obtained by Langer (1989a). This is likely to result from two effects, first from differences in the opacities used in the outermost layers. As shown by Langer, the predicted radii of WR stars are sensitive to C/O opacities. A second effect is the difference in the mean molecular weight mentioned above, since our models are evolutionary models. It has to be kept in mind that these radii are obtained imposing a hydrostatic structure and their comparison to observations may not be direct.

2.6. Mass vs. surface temperature

The surface temperature T_{\star} defined in Section 2.3 is shown in Fig. 3. It is related by Eqs. 2 and 4 using the Stefan–Boltzmann law. During the evolution in the WC/WO phase the surface temperature is in the range of 100000 – 150000 K and decreases very little (by less than 30%) compared to the luminosity and the radius. The final temperature increase at the end of He-burning is explained by the contraction (cf. above). Again, the

models with higher molecular weight have larger temperatures. The slightly wavy structure in Fig. 3 comes from the use of the triangle method (cf. Kippenhahn et al. 1967). The rather small uncertainties on the radii mentioned above, directly affect the surface temperature, since the luminosity remains unchanged.

2.7. Mass – T_{eff} relations

The effective temperature reflects the temperature at a certain optical depth in the wind. The values, as shown in Fig. 4, mainly occupy the range of 15000 to 40000 K. T_{eff} essentially depends on the mass loss rate \dot{M} , since the surface temperature varies very little during the WR stages. With the adopted mass-dependent mass loss rate we obtain a clear correlation between M and T_{eff} , shown in Fig. 4. WC/WO stars evolve towards higher temperatures, since as the stellar masses decline, the mass loss rate decreases and the wind becomes less opaque. Note the decrease of T_{eff} due to the wind by a factor of 10 to 4 with respect to the surface temperature.

WNE stars are found at larger T_{eff} because of their lower mass loss rates, which reduces the optical thickness of their winds. The WNE phase is shorter for more massive stars, hence not all models show up in this figure. The scatter among the models is a direct consequence of the variations of the surface temperature.

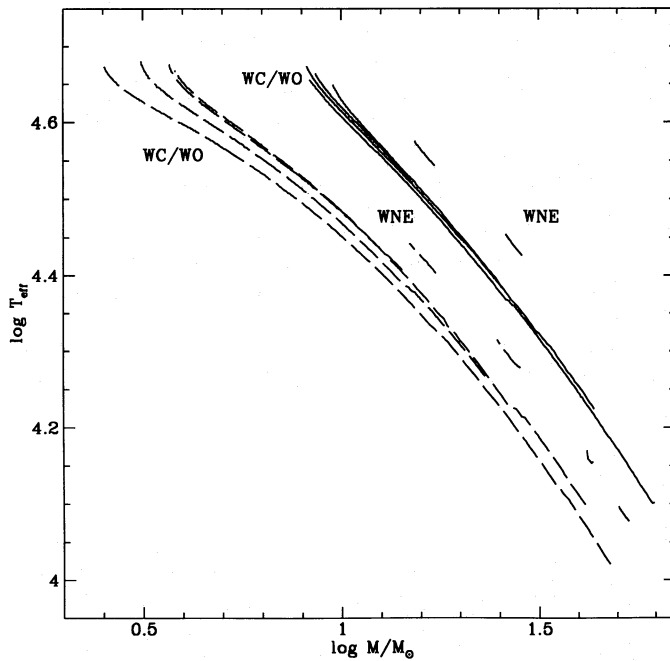


Fig. 4. Effective temperature of WNE and WC/WO stars. Models with “standard” mass loss (solid lines) and high M (long dashed lines) have different T_{eff} due to distinct optical thickness of the winds. The same holds for the separation between WNE and WC/WO stars

The effective temperature given by Schaller et al. (1992) takes electron- as well as line-scattering opacity into account. Thus T_{eff} cannot be compared to the temperature in continuum forming regions. If one modifies the velocity law and the terminal velocity assumed by Schaller et al. within the range of observed values (cf. Howarth & Schmutz 1992), T_{eff} varies only by a small amount of $\approx \pm 0.05$ dex. The uncertainties on the radii of the models have very little influence here. Since the absolute increase of the apparent radius (i. e. the optical-depth radius defined

in Section 2.3) only depends on the mass loss rate (cf. Langer 1989a) roughly speaking, larger radii would imply lower effective temperatures. However larger errors are to be expected from the adopted line force parameters. The inclusion of line opacities in the flux weighted mean opacity gives effective temperatures lowered by $\approx 0.1 - 0.2$ dex compared to pure electron scattering (cf. Maeder 1990).

For both mass loss rates considered, the following fits are obtained for the WC models:

$$\log T_{\text{eff}} = 4.9229 - 0.1152 \log \frac{M}{M_{\odot}} - 0.1918 \left(\log \frac{M}{M_{\odot}} \right)^2 \quad (5)$$

within ± 0.02 dex for standard \dot{M} , and

$$\log T_{\text{eff}} = 4.6642 + 0.085 \log \frac{M}{M_{\odot}} - 0.2757 \left(\log \frac{M}{M_{\odot}} \right)^2 \quad (6)$$

within ± 0.05 dex for $2 \cdot \dot{M}$.

With the adopted mass loss the WNE models are $\approx 0.05 - 0.08$ dex hotter than WC stars of the same mass.

2.8. Mass – mass loss relation

As an application of the relations derived so far, we can analyse the mass-dependent mass loss rate $\dot{M} \sim M^{2.5}$ given by Langer (1989b), which has been adopted for the WNE and WC/WO models by Schaller et al. Recently Howarth & Schmutz (1992) found a tight correlation between surface mass flux and their core temperature T_{\star} for the sample of WNE, WNL and WC stars. They state that $\dot{M}/R_{\star}^2 \sim T_{\star}^{\beta}$ with $\beta \approx 6$. If we identify their radii with ours and combine this with the M vs. R_{\star} and M vs. L relations given above, their correlation can be expressed as $\dot{M} \sim M^{\alpha}$ with $\alpha \in [1.8, 2.2]$ assuming reasonable error ranges for the relations used. This confirms the trend obtained from other observations (cf. Langer 1989b).

2.9. Luminosity – radius relation

The mass–luminosity (Eq. 2) and mass–radius (Eq. 4) relations can be combined to a L vs. R_{\star} relation. The following fit to our data is obtained within ± 0.1 dex:

$$\log \frac{R_{\star}}{R_{\odot}} = -1.8449 + 0.3382 \log \frac{L}{L_{\odot}} \quad (7)$$

This relation does of course not depend on mass loss.

2.10. Luminosity – T_{eff} relations

Figure 5 shows the HR–diagram for WNE and WC/WO tracks. All the characteristics have already been discussed in Sections 2.4 and 2.7. According to the mass loss of the models, the following fit is obtained for the WC phase:

$$\log \frac{L}{L_{\odot}} = -11.7763 + 10.2754 \log T_{\text{eff}} - 1.4239 (\log T_{\text{eff}})^2 \quad (8)$$

within ± 0.05 dex for standard \dot{M} , and

$$\log \frac{L}{L_{\odot}} = -53.3954 + 30.1082 \log T_{\text{eff}} - 3.8028 (\log T_{\text{eff}})^2 \quad (9)$$

within ± 0.2 dex for $2 \cdot \dot{M}$.

The WNE models have luminosities ≈ 0.2 dex higher at a given T_{eff} due to their lower mass loss rates for a given mass.

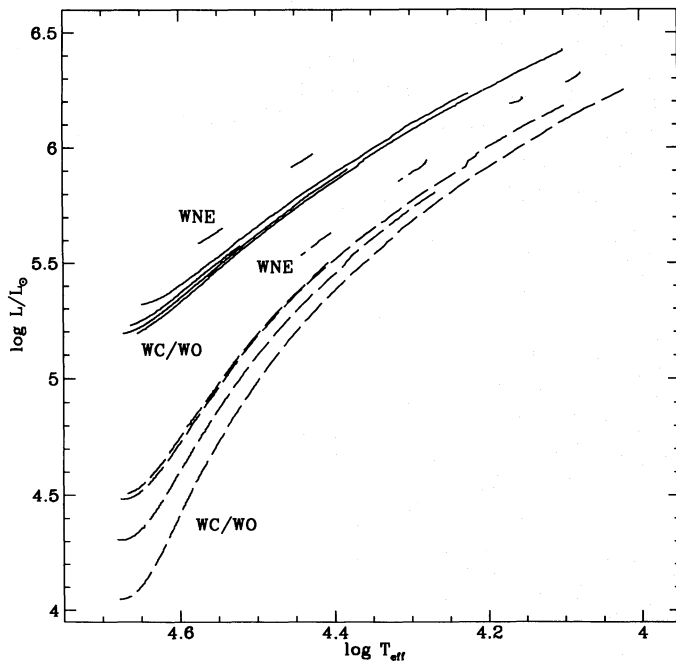


Fig. 5. HR-diagram of WNE and WC/WO stars. Models with “standard” mass loss (solid lines) and high \dot{M} (long dashed lines) are found at different T_{eff} due to distinct optical thickness of the winds. The same holds for the separation between WNE and WC/WO stars

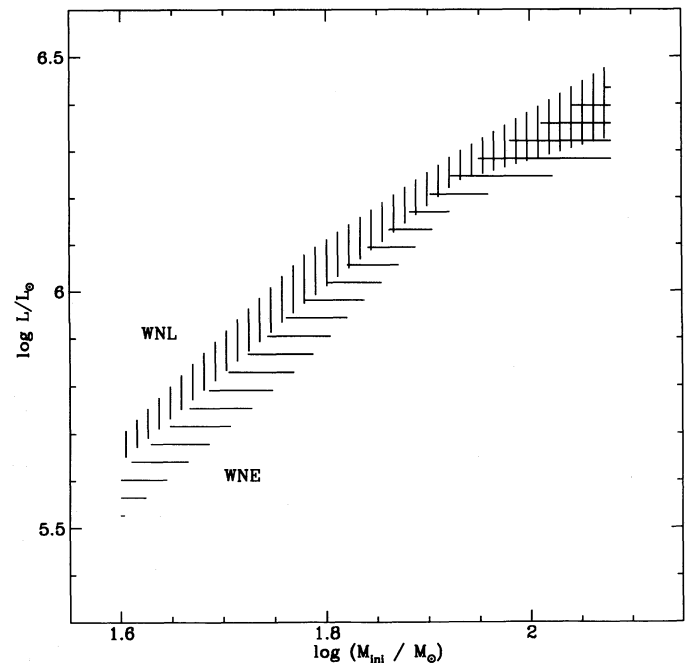


Fig. 6. Relation between initial ZAMS mass M_{ini} and luminosity of WNL (vertically shaded) and WNE stars (horizontally shaded) from models with both “standard” and high mass loss rates

2.11. WNL/WNE luminosity vs. initial mass

Since the mass loss rates during the WNL phase are not too large, the evolutionary tracks essentially predict constant luminosity during this phase for a given initial mass (cf. Schaller et al. 1992, Figs. 5, 7). Thus, given the luminosity of a WNL star, one can determine its initial ZAMS mass M_{ini} . Figure 6 shows the range of luminosities obtained from both models with “standard” and high mass loss rates. The spread remains quite small, since the different \dot{M} rates have not yet lead to significantly different actual masses for these objects.

Since the WNE phase is quite short, the luminosity of a given initial mass model in this phase spans quite a narrow range. Thus, the same type of relation as for the WNL phase between M_{ini} and L is obtained for WNE stars (see Fig. 6).

Of course, this relation can only be extrapolated down to the mass limit M_{WR} capable to form WR stars, which was found to be $25 < M_{\text{WR}}/M_{\odot} < 40$ by Schaller et al. The precise value of this mass limit is affected by mass loss in previous stages and thus by the evolutionary scenario which leads to WR star formation.

3. Chemical abundances and mass loss

An important prediction and test of evolutionary models are the surface abundances in all phases of stellar evolution. Models of WC and WO stars offer the unique opportunity to study the abundance of products of partial He-burning. Several effects determine the surface abundances of WR stars: The most important effect is mass loss in the post MS phase, since this essentially settles the moment the He-burning core gets rid of its envelope. The extension of the convective core also influences the abundances. For larger cores the products of He-burning will be revealed at an earlier stage of nuclear processing. Of course, other mixing

processes might be present in massive stars. Therefore the comparison of predicted He, C and O abundances with observations of WC/WO stars should give constraints on all these effects.

3.1. Abundances of WC/WO stars

To discuss the surface abundances the use of the ratio $(C + O)/\text{He}$ in number fractions is favoured in this context, since this quantity increases monotonically during He-burning. Figure 7 shows this value for all the models used here. Note that the stars evolve from higher towards lower luminosity until the end of He-burning. During the very short C-burning phase the luminosity increases again. This phase was not shown in the previous figures, since the relations derived are not valid at this stage. As an indication of the WC stage we also give the WC subtypes, classified by their surface abundances as suggested by Smith & Maeder (1991) (cf. also Smith & Hummer 1988).

As already mentioned above, the WC stage is marked by a relatively abrupt appearance of C and O. Thus at the beginning of this phase we obtain a lower limit for the C and O abundances (see Fig. 7), which then increase during further evolution. In models with higher initial mass, the core appears at an earlier stage of evolution, while the lowest mass (capable to form a WR star) produces higher surface abundances at a given mass resp. luminosity. At a closer look this working rule is somewhat confused by the detailed tracks in the HR-diagram, i. e. by the different BSG/RSG scenarios (cf. Schaller et al. 1992, Figs. 5, 7). This minimal limit for the C and O abundances in late WC stars provides valuable information on post MS mass loss rates and possible internal mixing processes.

If the surface abundance $(C + O)/\text{He}$ is taken as an indicator of the WC subtype (cf. Smith & Maeder 1991), we see that models with “standard” mass loss do not form any WC stars of subtype WC7 and later types, while models with the higher mass loss

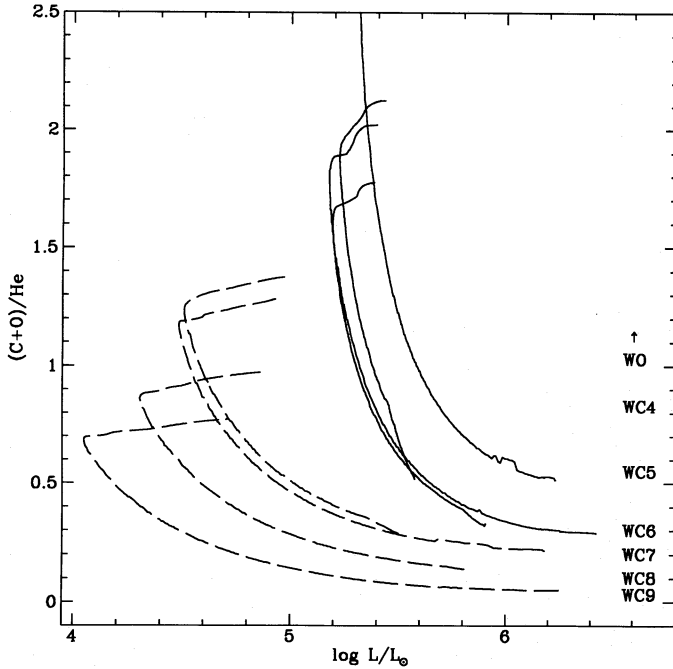


Fig. 7. Relative number abundances of carbon and oxygen to helium for WC/WO stars versus luminosity for models with “standard” mass loss (solid lines) and high \dot{M} (long dashed lines). Higher mass loss rates give lower C, O surface abundances. At low abundances the 120, 85, 60 and 40 M_{\odot} models are found from right to left with decreasing luminosity. WC subtypes according to Smith & Maeder (1991) are given on the right

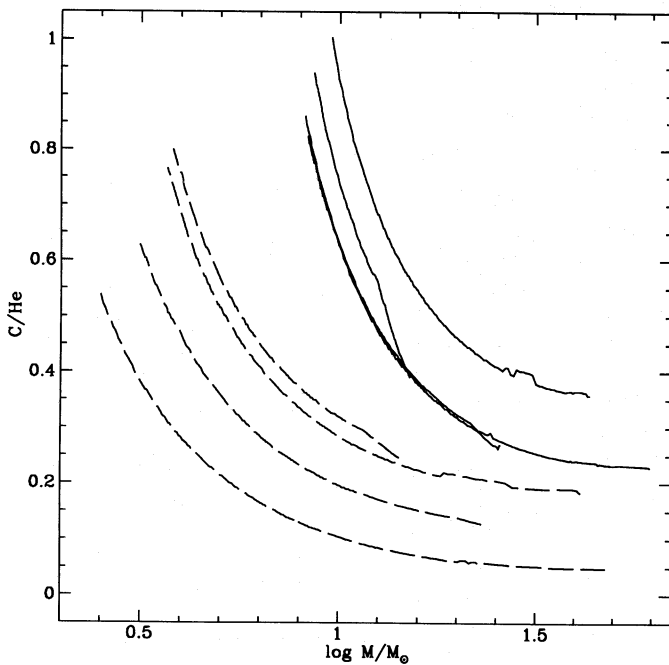


Fig. 8. Relative number abundance of carbon to helium for WC/WO stars versus mass for models with “standard” mass loss (solid lines) and high \dot{M} (long dashed lines)

rates also form WC9 stars and all earlier types. We recall in this context that WC9 stars are only found in the inner galactic regions where mass loss rates in phases preceding the WR stage are likely higher.

We will now compare the C and O abundances obtained from these two sets of models with observations and show further indications for larger post MS mass loss rates and/or other possible mixing processes. The comparison of abundances of WC/WO stars to observations is made difficult by the fact that detailed NLTE model-atmospheres including metals and a good knowledge of the ionisation balance are needed to achieve reliable spectroscopic determinations (cf. Hillier 1991). Therefore quite a small number of determinations have been made. One also has to keep in mind that different WC subtypes might be observed at different galactocentric distances, which could affect metallicity and hence mass loss rates (cf. Smith and Maeder 1991).

The carbon abundance of the evolutionary models during the WC and WO phase is given in Fig. 8. The lower limit of the C/He number abundance obtained from the models with higher mass loss is $C/He \gtrsim 0.05$, whereas adopting “standard” mass loss rates this limit is found to be $C/He \gtrsim 0.23$. However spectroscopic abundance determinations for WC stars given by Smith & Hummer (1988) and Nugis (1991) find carbon abundances with ratios $C/He \sim 0.1 - 0.7$ for WC9 to WC5-6 with increasing tendency from later WC subtypes to earlier ones.

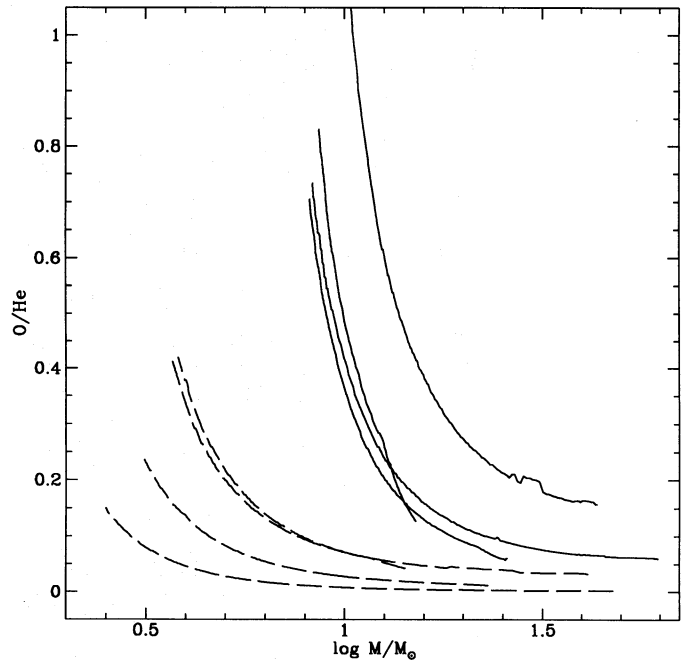


Fig. 9. Relative number abundance of oxygen to helium for WC/WO stars versus mass for models with “standard” mass loss (solid lines) and high \dot{M} (long dashed lines)

Figure 9 shows the oxygen abundance for both sets of models. As for the C abundance, assuming twice the “standard” post MS mass loss rates gives lower abundances, which agree well with the (few) values $O/He \sim 0.02 - 0.05$ obtained by Nugis (1991), who states a disagreement with the oxygen abundances obtained from evolutionary calculations. The determinations reviewed by Willis (1991) give $O/He \sim 0.01 - 0.1$ for WC/WO stars, again in good agreement with the models with larger mass loss rates.

The abundance ratio of oxygen to carbon (in numbers) for the models with standard \dot{M} is $0.2 \lesssim \text{O/C}$ up to $\text{O/C} \gtrsim 1$, where as for higher mass loss we obtain $\text{O/C} \sim 0.05 - 0.55$. The determinations by Nugis (1991) correspond to $\text{O/C} \sim 0.08 - 0.12$. Detailed modelling of one WC5 star by Hillier (1989) yields $\text{O/C} < 0.2$. From his $L = 10^5 L_\odot$ we obtain a mass of $M \approx 7 M_\odot$ from Eq. 2. Clearly only the models with higher \dot{M} are able to reproduce these abundances.

3.2. Higher mass loss rates ?

All the comparisons of observed surface abundances of WC/WO stars with the predictions by the models presented above, show that using “standard” mass loss rates and moderate overshooting the evolutionary models enter the WC/WO phase at too advanced a stage of nuclear processing. This suggests that stars should loose more mass in their post main-sequence phase before they become WC/WO stars. Of course one also has to consider other effects which might affect this result.

The models used in this work have been computed with a moderate overshooting of $d_{\text{over}}/H_p = 0.2$, which has been calibrated to the MS width for 1.25 to 25 M_\odot by Schaller et al. Overshooting affects the WC abundances mainly in two ways. First it slightly enlarges the core. Thus less mass in the envelope has to be peeled off to reveal the core and one obtains lower C and O abundances at the beginning of the WC phase. Another effect is to reduce the lifetime of the He-burning phase (cf. Maeder & Meynet 1987; Langer 1991), since this depends on the ratio of available fuel $q_{\text{cc}} M$ to the luminosity of the core $L \sim (q_{\text{cc}} M)^{1.7}$. In this case the core would be revealed in a more advanced evolutionary stage. Since our models have convective cores with mass fractions $q_{\text{cc}} > 0.5$ the first effect dominates. Thus models where the extension of the convective core is computed with the Schwarzschild criterion will show higher C and O abundances and less He in the WC/WO stages (cf. also Maeder & Meynet 1987). According to Langer (1989a), who computed some WR models with an increased convective core by one pressure scale height, the relative increase of the core mass fraction q_{cc} is 3–9% for 20 to 60 M_\odot models. Note that due to the larger temperature gradient, overshooting affects the core mass fraction less in the He-burning phase than on the MS. Thus in our models mass loss is more important than overshooting in determining the surface abundances of WC/WO stars.

Models computed with semiconvection by Langer (1991) have both smaller convective cores during He-burning and shorter lifetimes than ours. In this case the diffusive transport of C and O needs to be sufficiently effective to be able to reproduce the observed abundances at the beginning of the WC phase. Thus the lower limit of C and O abundances for late WC subtypes could give valuable information on the size of the He-burning cores and the efficiency of convection. Of course, additional mixing or diffusive processes which would modify the surface abundances may exist in massive stars, despite the fact that they have not yet been clearly identified.

Chemical evolution during He-burning relies on nuclear cross-sections, among which the $^{12}\text{C}(\alpha, \gamma)^{16}\text{O}$ rate is particularly uncertain and critical. We refer to Schaller et al. for a discussion of the nuclear reactions used in our models and justification of the adopted rate for the $^{12}\text{C}(\alpha, \gamma)^{16}\text{O}$ reaction. One has to keep in mind that the $^{12}\text{C}(\alpha, \gamma)^{16}\text{O}$ reaction rate has little influence on the abundances during a large time of He-burning, i. e. especially the lower limit for C and $(\text{C} + \text{O})/\text{He}$ in late WC subtypes is

hardly affected, since most of the emergent luminosity is provided by the 3α -process after the beginning of He-burning.

Comparing the lifetimes t_{WR} in the WR stage and the number ratios WR/O, WC/WR and WC/WN to observations can also serve as a test for evolutionary models. Previous studies by Maeder (1991) show remarkable agreement over various metallicities. Our models have somewhat shorter lifetimes for “standard” mass loss (cf. Schaller et al.). This also points in favour of higher rates.

To further analyse the question of post MS and WR mass loss rates, as well as the efficiency of convection and other possible mixing processes, it is of great importance to simultaneously determine the mass (or luminosity) and He, C and O abundances for observed WC/WO stars.

4. Conclusions

The relatively simple inner structure of WNE, WC and WO stars, which are quite generally accepted as bare stellar cores in the He-burning phase, determines most physical properties as a function of one main parameter, the mass of the bare core, and the chemical composition to a smaller extent. Therefore these properties are quite independent on the evolutionary scenario leading to such stars. This provides many interesting relations between WR parameters which are useful tools for the study of WR properties.

Based on new grids of stellar models by Schaller et al. (1992) we derived several relations for WNE, WC and WO stars between mass, luminosity, radius of the hydrostatic models and surface temperature and discussed some minor uncertainties (C/O opacities) which may influence the radii and surface temperatures. These relations are independent of the adopted mass loss rates. On the other hand, the effective temperature T_{eff} is mainly determined by the optically thick stellar wind, i. e. by the mass loss rate. With mass-dependent mass loss rates found by Langer (1989b) however, T_{eff} is also determined by the mass and can thus be related to the other quantities obtained above. As a word of caution one has to note that direct comparisons of the radii and T_{eff} with observations will suffer from some simplifications commonly adopted so far. All models are computed imposing a hydrostatic structure, grey atmospheres as the outer boundary conditions and evaluate T_{eff} a posteriori taking electron-scattering or a flux weighted mean opacity into account. Similarly, different definitions of radii and T_{eff} exist in models of WR atmospheres (cf. Baschek et al. 1991).

We obtained a relation between the initial ZAMS mass and the actual mass of WNL and WNE stars which hardly depends on the adopted mass loss rates. Furthermore, applying the relations derived above to the correlation between mass flux and temperature of WR stars recently obtained by Howarth & Schmutz (1992), we found additional indication for mass-dependent mass loss rates.

The appearance of He, C and O, as products of partial He-burning, on the stellar surface provides us with helpful information to understand some key points of post MS evolution of massive stars. Since the C and O abundances abruptly increase in models with large, growing He-cores, we obtain a lower limit for these abundances at the beginning of the WC phase which mainly depends on the adopted post MS mass loss rates, since this determines the time at which the envelope mass is lost. As a comparison models with semiconvection have very small cores and shorter lifetimes (cf. Langer 1991). Therefore, also depending

on the efficiency of the diffusive transport, different abundances and shorter WR lifetimes will be obtained.

Evolutionary models assuming “standard” mass loss rates and moderate overshooting (cf. Schaller et al. 1992) give higher abundances than obtained from spectroscopic determinations in WC stars. The amount of overshooting and the rather uncertain $^{12}\text{C}(\alpha, \gamma)^{16}\text{O}$ reaction rate have little influence on the lower abundance limit. Furthermore the comparison of lifetimes in the WR stages and observed number ratios of WN, WC and O stars also leads us to the suggestion that massive stars have up to ≈ 2 times larger post main-sequence mass loss rates than commonly adopted.

Reliable mass, He, C and O abundance determinations for WC and WO stars, precise post MS mass loss determinations and comparisons with evolutionary models will help to further clarify some dominant aspects of massive star evolution, as mass loss and internal mixing processes.

References

- Baschek B., Scholz M., Wehrse R., 1991, A&A 246, 374
 Chandrasekhar S., 1939, An Introduction to the Study of Stellar Structure, Dover Publ.
 Hamann W.R., Dünnebeil G., Koesterke L., Schmutz W., Wesolowski U., 1991, A&A 249, 443
 Hillier D.J., 1989, ApJ , 347, 392
 Hillier D.J., 1991, in Wolf-Rayet stars and Interrelations with Other Massive Stars in Galaxies, IAU Symp. 143, eds. K.A. Van der Hucht, B. Hidayat, Kluwer
 Howarth I.D., Schmutz W., 1992, A&A , in press
 Kippenhahn R., Weigert A., Hofmeister E., 1967, Methods in Computational Physics, 7, 129
 Lamers H.J.G.L.M., Maeder A., Schmutz W., Cassinelli J.P., 1991, ApJ 368, 538
 Langer N., 1989a, A&A 210, 93
 Langer N., 1989b, A&A 220, 135
 Langer N., 1991, A&A 252, 669
 Maeder A., 1983, A&A 120, 113
 Maeder A., 1985, A&A 147, 300
 Maeder A., 1990, A&AS 84, 139
 Maeder A., 1991, A&A 242, 93
 Maeder A., Meynet G., 1987, A&A 182, 243
 Nugis T., 1991, in Wolf-Rayet stars and Interrelations with Other Massive Stars in Galaxies, IAU Symp. 143, eds. K.A. Van der Hucht, B. Hidayat, Kluwer
 Schaller G., Schaerer D., Meynet G., Maeder A., 1992, A&AS in press
 Schmutz W., Schaerer D., 1992, in Atmospheres of Early-type Stars , eds. U. Heber, C.S. Jeffery, Lecture Notes in Physics 401, Springer-Verlag
 Smith L.F., Hummer D.G., 1988, MNRAS 230, 511
 Smith L.F., Maeder A., 1991, A&A 241, 77
 Willis A.J., 1991, in Evolution of Stars: the photospheric abundance connection, IAU Symp. 145, eds. G. Michaud, A. Tutukov, Kluwer